The Astrophysical Journal, 640:971–981, 2006 April 1

ASTROMINERALOGY OF THE 13 μm FEATURE IN THE SPECTRA OF OXYGEN-RICH ASYMPTOTIC GIANT BRANCH STARS. I. CORUNDUM AND SPINEL

Kyle DePew, Angela Speck, and Catharinus Dijkstra
Department of Physics and Astronomy, University of Missouri, Columbia, MO 65211; kdd264@mizzou.edu
Received 2005 September 30; accepted 2005 November 29

ABSTRACT

Asymptotic giant branch (AGB) stars have several interesting infrared spectral features. Approximately half the oxygen-rich AGB stars to be investigated spectroscopically exhibit a feature at $\sim$13 μm. The carrier of this feature has not yet been unequivocally identified but has been attributed to various dust species, including corundum (α-Al_2O_3), spinel ($MgAl_2O_4$), and silica (SiO_2). In order to constrain the carrier of the 13 μm feature, we have used the one-dimensional radiative transfer code DUSTY to model the effects of composition and optical depth on the shape and strength of the emerging 13 μm feature from corundum and spinel grains. We have modeled various corundum, spinel, corundum-silicate, and spinel-silicate mixtures in dust shells surrounding O-rich AGB stars. These models demonstrate that (1) if corundum is present in these circumstellar dust shells, even at very low relative abundances, a $\sim$13 μm feature should be observed; (2) corundum's weak $\sim$21 μm feature will not be observed, even if it is responsible for the $\sim$13 μm feature; (3) even at low relative abundances, spinel exhibits a feature at 16.8 μm that is not found in observations; and (4) the grains must be spherical. Other grain shapes (spheroids, ellipsoids, and hollow spheres) shift the features to longer wavelengths for both spinel and corundum. Our models show that spinel is unlikely to be the carrier of the 13 μm feature. The case for corundum as the carrier is strengthened but not yet proven.

Subject headings: circumstellar matter — dust, extinction — infrared: stars — stars: AGB and post-AGB — stars: mass loss

1. INTRODUCTION

Low- to intermediate-mass stars (0.8–8 $M_\odot$) ascend the AGB branch phase toward the end of their lives. During this period, the star is comprised of a carbon core surrounded by hydrogen- and helium-burning shells. Stellar pulsations lead to mass loss. As material drifts away from the star, it cools and can condense into dust grains. In this way a star expels gas including the newly formed heavier elements into its surroundings, giving rise to a circumstellar shell of dust and gas. Convection currents inside the star dredge up material from the helium- and hydrogen-burning shells to the surface of the star. Among the heavier elements ejected are large amounts of carbon and oxygen. Because carbon monoxide (CO) is a very stable molecule and forms very easily in such environments, carbon and oxygen atoms combine into CO, leaving the more abundant element to dominate the chemistry. Stars start their lives with cosmic C/O ($\approx$0.4) and thus have oxygen-rich chemistry. In some cases, the dredge-up of newly formed carbon is efficient enough to raise C/O above unity and become carbon-rich. The chemistry dictates the mineralogy of the dust shell, which can be studied using spectroscopic and meteoritic data. Minerals absorb light radiated by the star and reemit in the infrared (IR) range. Composition, crystal structure, grain size, and morphology all affect the resulting IR spectrum, as do the temperature and density distribution in the dust shell. We can compare laboratory spectra of different dust species to astronomical observations in order to match and identify the dust species present in circumstellar envelopes. Furthermore, we can use radiative transfer modeling to assess the effects of the temperature and density distribution (optical depth) within these circumstellar envelopes.

1.1. *Dust Features around* O*-rich AGB Stars*

In the late 1960s, while investigating deviations of stellar energy distributions from blackbodies, Gillett et al. (1968) discovered a peak near 10 μm in the spectra of four late-type, evolved, variable stars. Woolf & Ney (1969) attributed this emission peak to circumstellar amorphous silicate. Since then there has been much interest in the exact nature and formation of the dust grains around cool evolved stars.

Various attempts have been made to classify the observed dust features of oxygen-rich (O-rich) evolved stars (e.g., Little-Marenin & Little 1990; Sloan & Price 1995; Speck et al. 2000). All these authors have classified the observed spectra into groups according to the shape of the dust feature, which reflects a progression from a broad feature to the classic narrow 10 μm silicate feature. This progression of the spectral features is expected to represent the evolution of the dust from the early forming refractory oxides (the broad feature) to the dominance of magnesium-rich silicates (the narrow 10 μm feature). An alternate explanation for this sequence actually reverses the time series. In this case the condensation sequence is determined by the precise C/O ratio. Stars with relatively low C/O would exhibit strong silicate features, while stars with higher C/O ratios (but still $<$1) could have spectra dominated by Al_2O_3 (Sloan & Price 1998). However, recent studies of O-rich AGB stars in both the Milky Way and in the Large Magellanic Cloud support the former scenario (Heras & Hony 2005; Dijkstra et al. 2005).

1.1.1. *The* 13 μm *Feature*

Vardya et al. (1986) observed 20 Mira variable stars using the *Infrared Astronomy Satellite* (*IRAS*; Neugebauer et al. 1984) Low Resolution Spectrograph (LRS) and found a previously unnoticed feature peaking between 12.5 and 13 μm. Vardya et al. (1986) subsequently attributed this feature to some sort of silicate. This feature was later found to be specifically associated with O-rich AGB stars (Sloan & Price 1995). Further analyses of *IRAS* LRS (Little-Marenin & Price 1986; Little-Marenin & Little 1988, 1990; Sloan & Price 1995; Sloan et al. 1996), and *Infrared Space Observatory* (*ISO*; Kessler et al. 1996) Short

Wavelength Spectrometer (SWS; de Graauw et al. 1996) observations (Justtanont et al. 1998; Posch et al. 1999; Fabian et al. 2001; Sloan et al. 2003), as well as analysis of ground-based spectra (Speck et al. 2000), have yielded several possible carrier materials for the feature, but as yet none has been conclusively identified.

The 13 μm feature has several interesting characteristics that must all be explained by any carrier candidate. First, given that it appears solely in O-rich stars, the carrier species is likely to be an oxide or silicate of some sort. It has also been observed that only about half of all AGB stars possess this feature, and of those, $\sim$75%–80% of semiregular variable (SR) stars, $\sim$20%–25% of Mira variables, and virtually no supergiants exhibit it (Sloan et al. 1996; Speck et al. 2000). The dust shells of SRs are generally optically thinner than those of Mira variables (e.g., Marengo et al. 2001). However, the classifications of SRs and Mira variables are not necessarily fixed throughout the AGB phase of any given star. It is possible that SRs evolve into Mira variables (e.g., Feast & Whitelock 1987). It is also possible that stars go through alternating periods in which they would be identified successively as Mira variables and SRs (Kerschbaum & Hron 1992). Therefore, the 13 μm feature is either produced by a mineral species of low relative abundance whose spectral features are overwhelmed by those of the surrounding dust as optical depth increases, or the carrier mineral is only formed in a relatively low density environment and not in a relatively high density environment. The 13 μm feature is also correlated with features at 10, 20, and 28 μm, as well as CO_2 emission lines (Begemann et al. 1997; Justtanont et al. 1998; Speck et al. 2000; Sloan et al. 2003). This feature is always seen in emission and has never been observed in absorption.

Over the years, various possible sources of the feature have been proposed. Onaka et al. (1989) suggested aluminum oxide (alumina; Al_2O_3) as the source of the 13 μm feature, while it was later suggested that the aluminum oxide might be in the form of corundum (α-Al_2O_3; Glaccum 1995). Begemann et al. (1997), in their laboratory analysis of corundum, showed that in addition to the 13 μm feature, corundum possesses a weak feature at $\sim$21 μm. Since this $\sim$21 μm feature has not been observed in the spectra of astronomical sources that exhibit the 13 μm feature, Begemann et al. (1997) concluded that corundum could not be the carrier of the 13 μm feature. Begemann et al. (1997) also found a correlation between the 13 μm feature and the classic 10 μm silicate feature and thus concluded that the carrier of the 13 μm feature must be some sort of silicate. However, Posch et al. (1999) stated that the strong 10 μm Si-O feature is not observed in the *IRAS* or *ISO* spectra of AGB stars that exhibit the 13 μm feature, contradicting the finding of Begemann et al. (1997). Kozasa & Sogawa (1997a, 1997b) proposed grains consisting of Al_2O_3 cores and silicate mantles for the carrier of the 12.5–13.0 μm feature. However, this was investigated by Posch et al. (1999), who found that (1) there would have to be a large population of grains of $\sim$85% Al_2O_3 and (2) there would have to be an even larger number of pure silicate particles to produce anywhere near the correct ratio of 13 μm to 10 μm flux strengths. They therefore concluded that such core-mantle grains were unlikely to be the carriers of the 12.5–13.0 μm feature.

Posch et al. (1999) suggested spinel ($MgAl_2O_4$) as the carrier of the 13 μm feature. The stoichiometric natural spinel also exhibits features at 16.8 and 32 μm. Posch et al. (1999) suggested that both the 16.8 and 32 μm features are observed in *ISO* SWS data for O-rich AGB stars that exhibit the 13 μm feature. However, Sloan et al. (2003) pointed out that the observed 16.8 μm feature is too narrow to be a dust feature and suggested it may instead be explained by the presence of CO_2, which is well correlated with the 13 μm feature (Justtanont et al. 1998). Furthermore, they found no evidence for a 32 μm feature. Further studies of the *ISO* SWS spectra for stars that exhibit the 13 μm feature by Heras & Hony (2005) also failed to find a dust feature to match the spinel 16.8 μm spectral feature.

Silica (SiO_2) was first suggested as the carrier of the 13 μm feature by Speck (1998). Silicon dioxide is an anomaly among the oxides. Although SiO_2 is chemically an oxide, the structures and properties of the silica minerals are more closely allied to those of silicates (see Speck 1998). Posch et al. (1999) claimed that the lack of correlation between the 13 μm feature and the strong $\sim$10 μm expected for SiO_2 should rule silica out as the carrier. However, as stated above, Begemann et al. (1997) did find a correlation between the 13 μm feature and the classic 10 μm silicate feature and thus concluded that the carrier of the 13 μm feature must be some sort of silicate (which could include silica). It is possible that the Posch et al. (1999) objection was based on unusual optical constants. The SiO_2 constants (from Henning & Mutschke 1997) produce an emission feature that is shifted to the blue side of the regular silicate feature. This is not seen for other SiO_2 optical constants (e.g., Spitzer & Kleinman 1961). Furthermore, silica has several possible crystal structures, each of which has a subtly different spectrum, such that the ratio of feature strengths of the $\sim$10 and 13 μm features vary substantially (see Speck 1998). A detailed analysis of the possibility of silica being the carrier of the 13 μm feature, and the implications of such a finding, will be presented in a forthcoming paper (K. DePew et al. 2006, in preparation).

1.2. *Presolar Grains*

For information beyond what spectroscopy can provide us, meteoritic analysis can provide detailed information on circumstellar dust grains (see, e.g., Clayton & Nittler 2004; Hoppe 2004). The isotopic compositions of presolar grains indicate that they originated outside the solar system. Al_2O_3 and spinel grains have been found in meteorites (Nittler et al. 1994a, 1994b, 1997; Huss et al. 1994) and have isotopic signatures that suggest they were formed around oxygen-rich AGB stars.[1]

Thus, presolar grains provide laboratory samples of circumstellar oxides that can be studied in the laboratory. Examining presolar material is also useful in setting limits on the grain size and structure of the minerals that form around evolved stars. Presolar Al_2O_3 grains have sizes in the range 0.5–5 μm (Nittler et al. 1997), while the presolar spinel grains are typically smaller (0.2–0.5 μm; Zinner et al. 2003). Only two alumina grains have been studied crystallographically (although many have been studied isotopically), one amorphous and the other crystalline (Stroud et al. 2004). The crystal structure of the spinel presolar grains is not known. Clearly more crystallographic data are needed for comparison for observational evidence for these dust species. Furthermore, the scanning electron microscope images of presolar spinel and corundum grains suggest that these grains are not spherical and not fluffy. However, the presolar sample only preserves the hardiest grains and may not be representative of the entire range of grain shapes forming in the outflows of AGB stars.

1.3. *Purpose*

In this paper we investigate what compositions of dust would exhibit the 13 μm feature and set limits on the range of

[1] While many of the published articles on presolar Al_2O_3 grains refer to them as corundum, the majority of them have unknown crystal structures and should be referred to as alumina (Hoppe 2004).

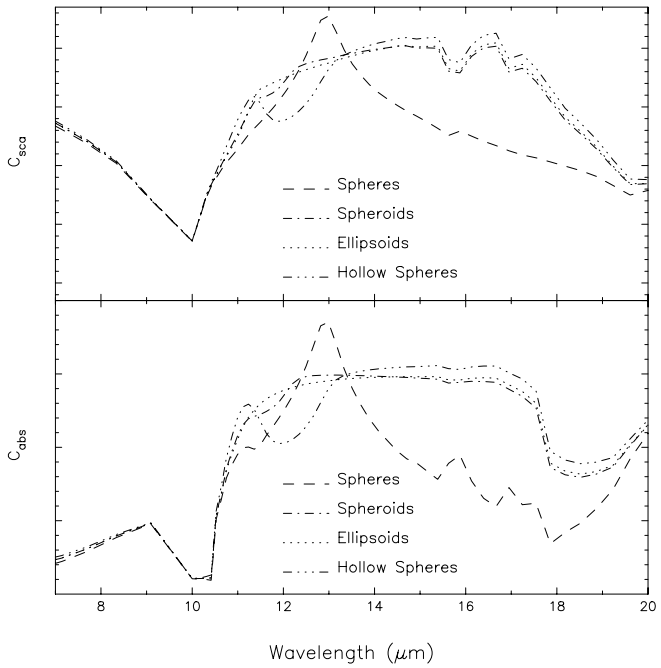

FIG. 1.—Scattering and absorption cross sections of corundum showing the effects of different grain shapes. *Top*: Scattering cross section in square centimeters. *Bottom*: Absorption cross section in square centimeters.

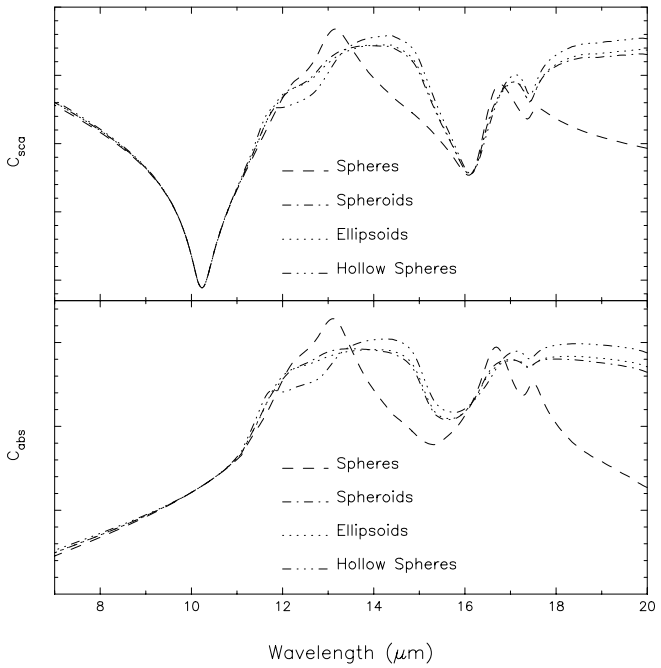

FIG. 2.—Same as Fig. 1, but for stoichiometric spinel.

compositions and grain morphologies that would best fit the observed spectra. To do so, we employ the one-dimensional radiative transfer model DUSTY (Nenkova et al. 2000) and calculate the scattering and absorption cross sections for different grain shape distributions following Min et al. (2003). Section 2 discusses the effects of grain shape distributions on the spectra expected from corundum and spinel. Section 3 outlines the DUSTY models we have produced, and the results of this modeling are presented in § 4. The implications of these models are discussed in § 5.

2. GRAIN SHAPE AND SIZE

We investigate the effect of grain shape on the spectral features of corundum and spinel. To this end, we have calculated the scattering coefficients of corundum and natural and artificial spinels for spherical, spheroidal (oblate or prolate), and ellipsoidal grains. Moreover, we also consider hollow spheres. Although these calculations did not employ mixtures of different mineral species, it was sufficient to show the significance of the grain shape in determining the output spectrum.

For spherical particles, we used Mie theory. However, for spheroids, ellipsoids, and hollow spheres, we follow Bohren & Huffman (1983) and Min et al. (2003). In this case, the grains are assumed to be small compared to the wavelengths of interest ($a \ll \lambda/2\pi$), and the particles in a given grain shape distribution are volume equivalent.

In the case of hollow spheres, it is assumed that spherical grains are made up of spherical shells with vacuum inclusions. Min et al. (2003) found that a continuous distribution of hollow spheres, although not suspected of representing the real shape of circumstellar grains, is more successful in reproducing the observed spectra of a distribution of irregularly shaped particles than other grain shape distributions. Therefore, these particles are used as a proxy for fluffy dust grains.

Figures 1 and 2 show the effects of varying the grain shapes for corundum and spinel, respectively. The spectral features of both corundum and spinel are shifted to the longer wavelengths if the grains are not spherical. For spinel, both spheroidal and ellipsoidal grains cause the scattering cross section of the 13 μm feature to be reduced by about one-half relative to the spherical grain feature. Furthermore, the peak is shifted about 0.5 and 1.0 μm to 13.5 and 14.0 μm for spheroids and ellipsoids, respectively. The wavelength shift for hollow spheres is even more noticeable. Here the peak is shifted almost to 14.5 μm. When we change the grain shape from spherical, the 13 μm feature of corundum exhibits a cross-section reduction of one-half with a relatively consistent 1 μm (longward) shift for all nonspherical grain shapes. Furthermore, the weak 20.5 μm feature seen in the spectrum for spherical corundum grains is shifted to $\sim$22 μm and is much stronger once the grains are assumed to be nonspherical. This shows that neither corundum nor spinel would produce a 13 μm feature for any grain morphology other than spherical. The implications of the need for spherical grains is discussed in § 5.

The effect of grain shape and aluminum content on spinel's IR spectrum was investigated by Fabian et al. (2001), who concurred that it is necessary for the grains to be spherical in order for the feature to appear at 13 μm. Furthermore, they found that the composition of the spinel needed to be almost stoichiometric and got their best match to the observed feature using a natural sample of spinel. The implications of this are discussed further in § 5.

3. RADIATIVE TRANSFER MODELING WITH DUSTY

Using the one-dimensional radiative transfer code DUSTY (Nenkova et al. 2000), we have modeled circumstellar dust shells of varying compositions and optical depths. In all cases the star is assumed to be a 3000 K blackbody, while the inner dust shell temperature (T_{in}) was fixed at 800 K. Speck et al. (2000) showed that varying the adopted blackbody temperature by $\pm$1000 K about the adopted 3000 K had very little effect on the shape and strength of the derived continuum-subtracted dust features. Therefore, the natural scatter of expected stellar temperatures should not have a large effect on our models. However,

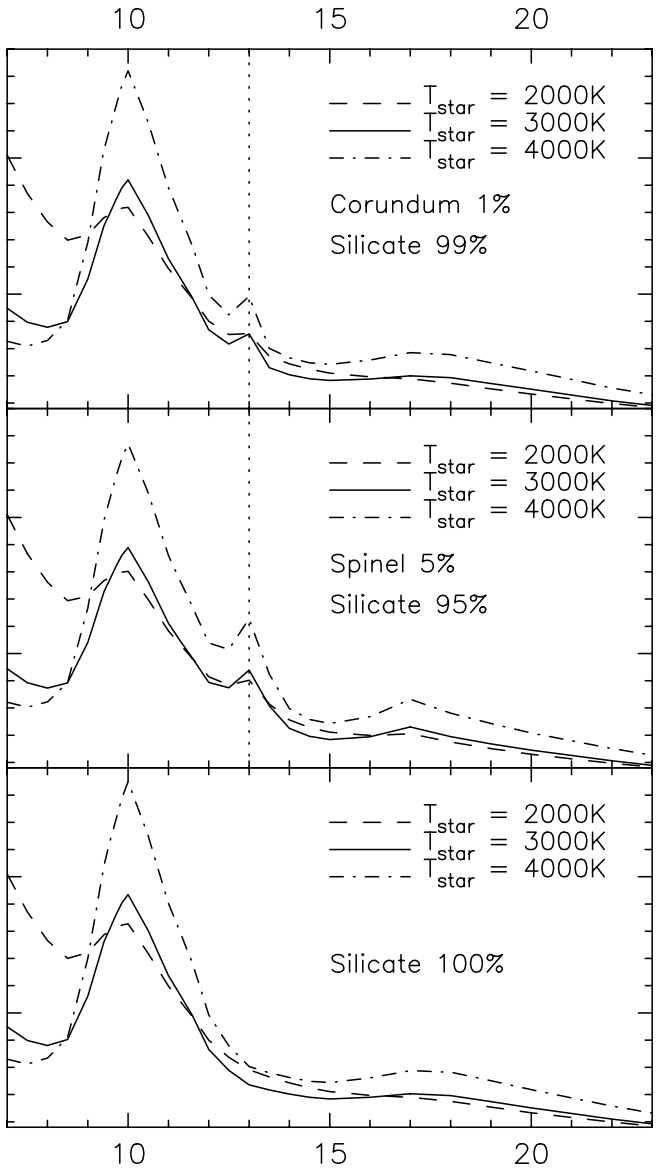

FIG. 3.—Effect of stellar temperature on the shape, position, and relative strengths of IR dust features: *top*, 1% corundum, 99% warm silicate; *middle*, 5% spinel, 95% warm silicate; *bottom*, 100% warm silicate. The dotted line indicates the location of the peak of the 13 μm feature.

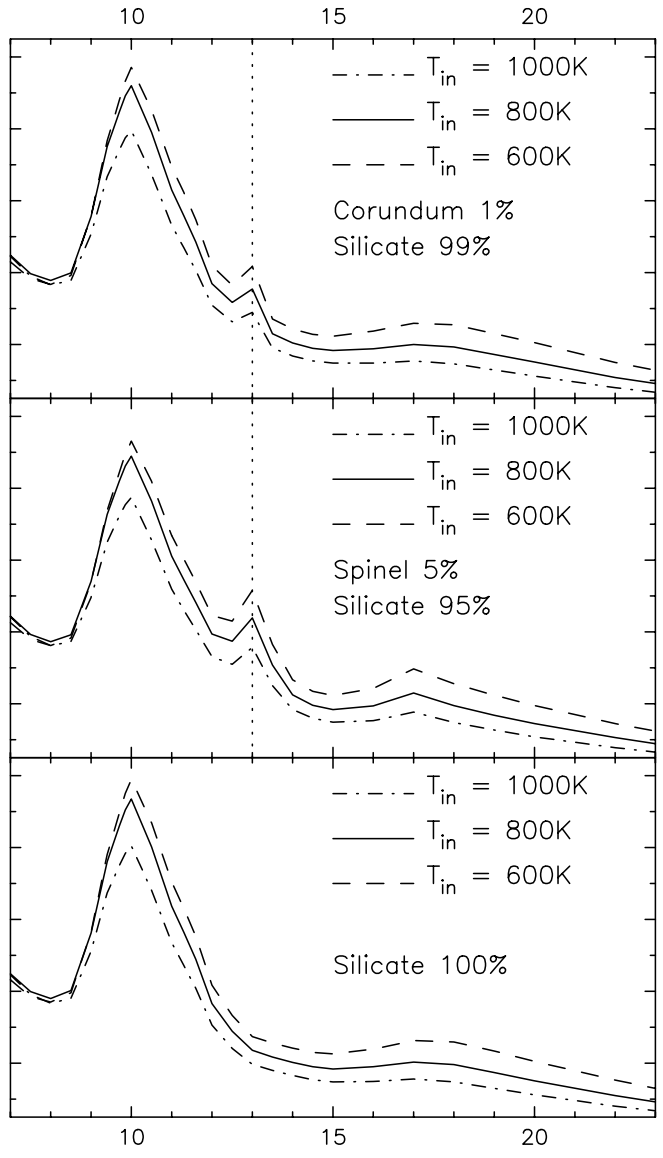

FIG. 4.—Same as Fig. 3, but for the effect of dust condensation temperature (i.e., dust temperature at the inner radius on the circumstellar shell).

models with $T_* = 2000$ and 4000 K are presented in Figure 3 to demonstrate that the stellar temperature is not a major effect in our modeling. The overall shape of the spectrum, and in particular the positions and the ratios of strength of different features, remain constant, demonstrating that our models are not very sensitive to the stellar temperature. The value $T_{\rm in} = 800$ K was used because these spectra are generally dominated by amorphous silicates. Dust condensation at temperatures $\gtrsim$1000 K leads to the formation of crystalline silicates (e.g., Tielens et al. 1997; Tielens 1990). Furthermore, it has been shown that the carrier of the classic 9.7 μm feature must be "dirty," i.e., that the olivine composition contains iron, rather than being the pure magnesium endmember. This also implies formation below 1000 K (e.g., Tielens et al. 1997; Tielens 1990). Efficient dust formation will only occur within a range of temperatures (600 K $\lesssim T_{\rm cond} \lesssim$ 1200 K; Sedlmayr 1997). In addition, Lodders & Fegley (1999) have shown that dust condensation temperatures vary over several hundred degrees for the range of gas pressures expected in the dust formation regions of AGB stars. Therefore, the precise value for $T_{\rm in}$ is negotiable. In order to determine the effect of this parameter we have produced models in which $T_{\rm in}$ was varied. The resulting models are shown in Figure 4. It is clear from our models that variations in $T_{\rm in}$ do not have a big impact on either the peak positions of the dust features or on the ratios of their strengths. In these models, the refractory grains (corundum or spinel) and silicate are assumed to be cospatial and have identical grain-size distributions. The refractory grains are unlikely to have the same grain-size distributions as the more abundant, lower temperature condensates (e.g., silicates). Furthermore, refractory grains form at a higher temperatures than silicate and thus should be represented by a higher $T_{\rm in}$. (Our range in $T_{\rm in}$ is representative for silicate grains.) In this way, we might expect the structure of the dust shell to be such that a thin inner shell of refractory oxides is surrounded by a larger, cooler shell of (mostly) silicate. These effects cannot be modeled using DUSTY and thus are beyond the scope of the present work. However, Figure 4 shows that the peak position of the 13 μm feature is not very sensitive to $T_{\rm in}$. The inner dust temperature affects the brightness of the feature. If we were to view a 13 μm feature emanating

TABLE 1
MODELS

Mineral Name	Mineral Formula	Reference
Corundum	Al_2O_3	Gervais (1991)
Spinel	$MgAl_2O_4$	Fabian et al. (2001)
Amorphous alumina	Al_2O_3	Begemann et al. (1997)
Warm silicates	"SiO_4"	Ossenkopf et al. (1992)

from the inner part of the dust shell, through the optically thin silicate shell, we would still expect to see the feature. The brightness of the feature relative to the silicate feature may change, being either brighter because the oxide grains are hotter, or fainter because of a small amount of absorption by the outer shell. Therefore, our cospatial dust grains are legitimate for providing constraints on the carrier of the 13 μm feature.

For the DUSTY modeling, we assume the dust grains are spherical. While it is possible to synthesize radiative transfer models for nonspherical grains, our analysis of the effect of grain shapes shows that nonspherical grains of either corundum or spinel would not have a 13 μm feature (see § 2). Another side effect of the differing condensation temperatures for the oxides and silicates is that we might expect there to be dust grains comprised of an oxide core and a silicate mantle (e.g., Salpeter 1974; Kozasa & Sogawa 1997a, 1997b). In this case, the thickness of the silicate mantle will change with grain growth, so that we would expect a grain distribution in which the silicate mantle is thicker at greater distances from the star. While effective medium theory can produce the absorption and scattering cross sections for core-mantle grains, which can then be used in DUSTY, the expected change in mantle thickness as a function of location in the dust shell, makes the value of its implementation debatable. Furthermore, Posch et al. (1999) showed that core-mantle grains are unlikely to be the carrier of the 13 μm feature. Thus, core-mantle grains are beyond the scope of the present work.

It has been shown that using a radial dust density distribution of $1/r^2$ can reproduce the IR spectra of AGB stars reasonably well (Rowan-Robinson & Harris 1982, 1983a, 1983b). Therefore, the adopted radial density profile of the circumstellar shell is $1/r^2$. We assume an MRN (Mathis et al. 1977) grain size distribution [i.e., $n(a) \propto a^{-q}$, where n is the number of grains in the size interval $[a, a + da]$ and $q = 3.5$; $a_{\min} = 0.005$ μm and $a_{\max} = 0.25$ μm]. For the composition of the grains, we have chosen to use warm silicates together with either corundum or spinel. Following Speck et al. (2000) and Maldoni et al. (2005), we have also used amorphous alumina. The optical constants for corundum and spinel were drawn from Gervais (1991) and Fabian et al. (2001), respectively. For those constants corresponding to warm silicates and amorphous alumina, the optical constants came from Ossenkopf et al. (1992) and Begemann et al. (1997), respectively. Table 1 summarizes the provenance of the optical constants used in this study.

The primary optical depth used was $\tau_{10\ \mu m} = 0.05$, relevant to the circumstellar shells of Mira variables and SRs (Ramdani 2003). However, it is known that there are variations in the optical depth of Mira variables and SRs, and therefore, we have modeled a range of optical depths. While most Mira variables and SRs are expected to be more or less optically thin in the late stages of the AGB phase, optical depth is expected to increase rapidly. We have therefore constructed models with a wide range of optical depths in order to investigate the conditions under which the observed 13 μm feature may appear.

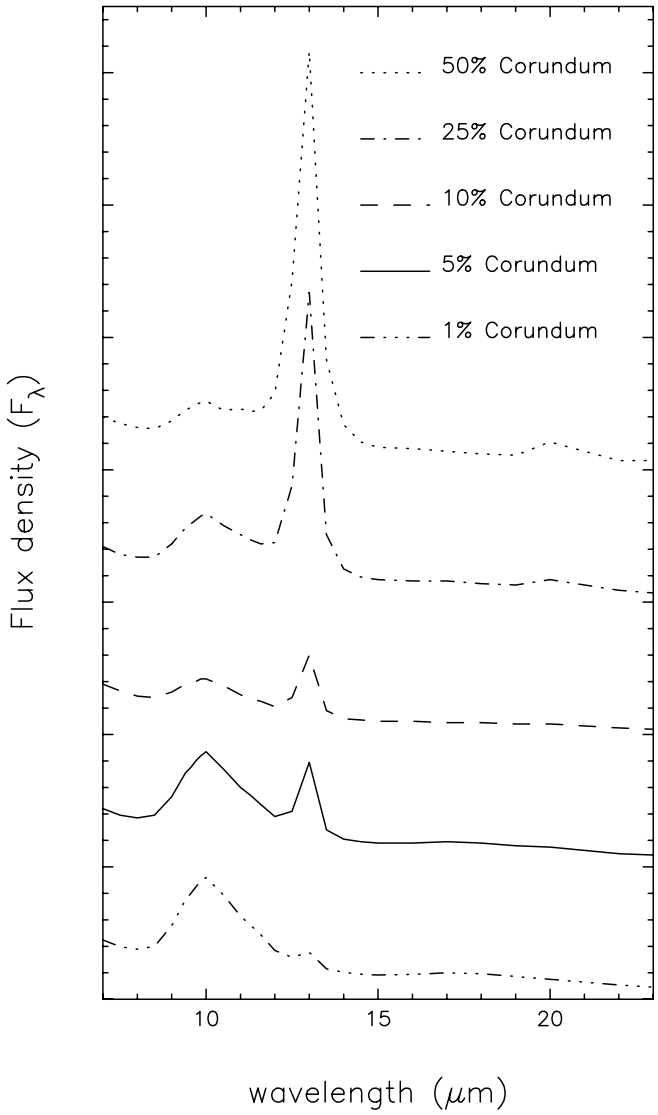

FIG. 5.—Model 7–23 μm spectra for different mixtures of corundum and warm silicates at fixed optical depth ($\tau_{10\ \mu m} = 0.05$). In each case the dust composition is given by the percentage of corundum, with the remainder of the dust comprised of warm silicates only.

For the modeling of the effect of composition changes, the dust species being investigated were added to a dust shell consisting of warm amorphous silicates. Speck et al. (2000) showed that even stars that exhibit spectral features tentatively attributed to oxides still need some contribution from amorphous silicates to match the blue side of the spectral features in the 10 μm region. We also ran models without any silicate, but including both amorphous alumina and corundum, in order to test the results of Speck et al. (2000) and to model astronomical spectra in which silicate emission is either weak or apparently nonexistent. In addition, this allows us to test the hypothesis that corundum grains could be hidden by the formation of amorphous alumina dust as circumstellar densities increase.

4. RESULTS

4.1. *Corundum*

Figure 5 shows the model spectra for mixtures of corundum and warm silicates, with the optical depth held constant at $\tau_{10\ \mu m} = 0.05$. As the relative abundance of corundum is reduced, the 13 μm feature of corundum is seen to gradually

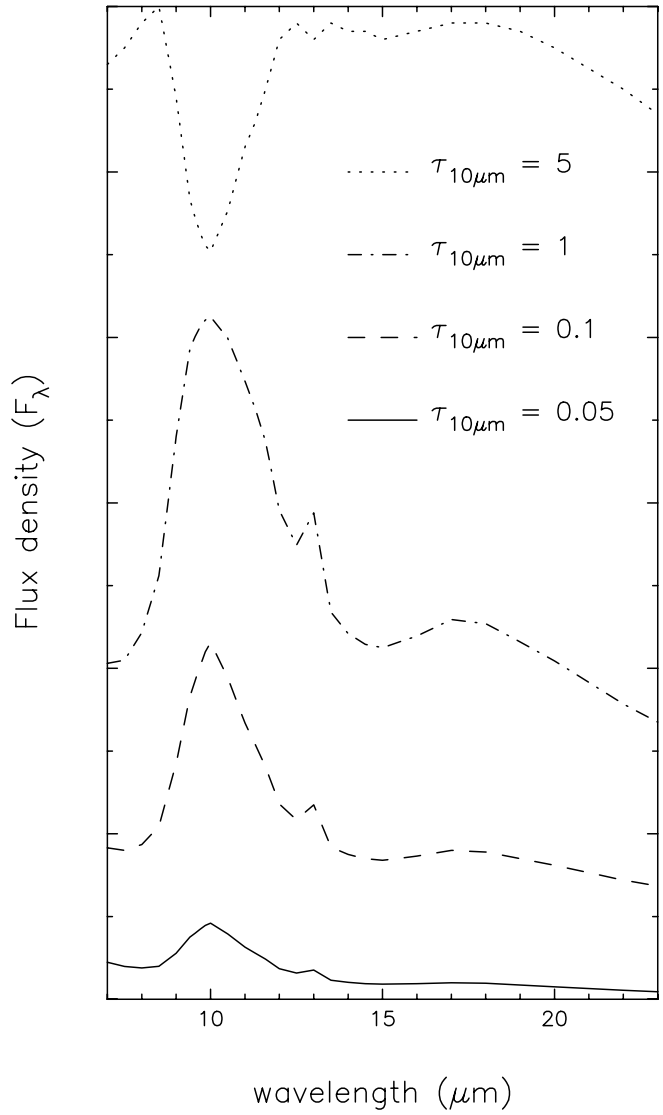

FIG. 6.—Model 7–23 μm spectra for a fixed mixture of corundum (1%) and warm silicates (99%) at different optical depths.

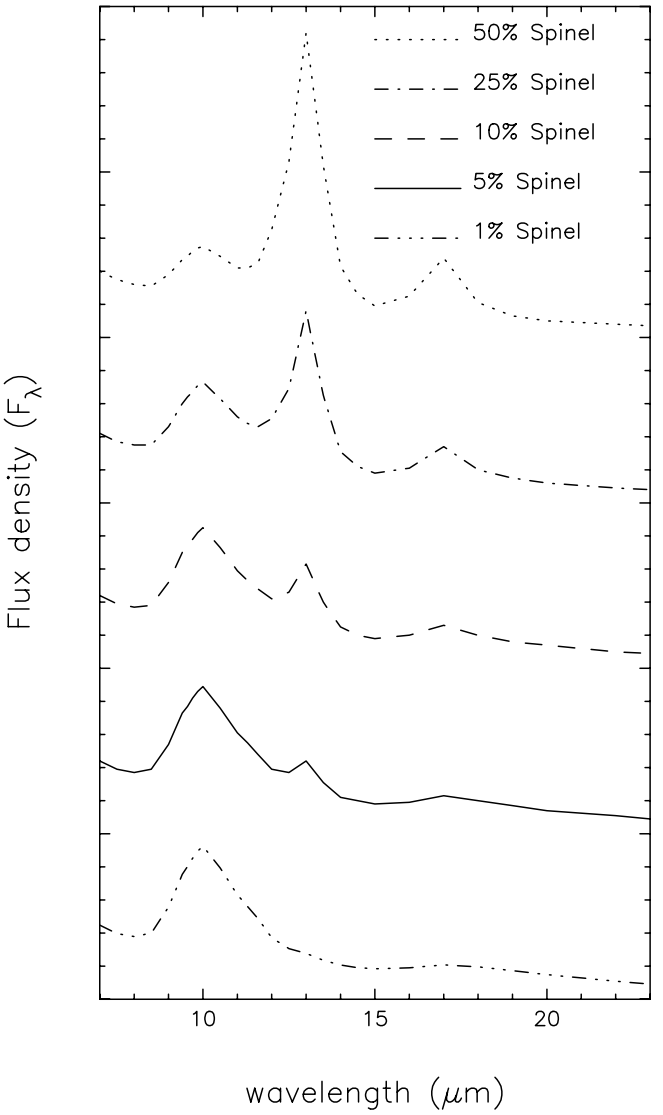

FIG. 7.—Model 7–23 μm spectra for different mixtures of spinel and warm silicates at fixed optical depth ($\tau_{10\ \mu m} = 0.05$). In each case the dust composition is given by the percentage of spinel, with the remainder of the dust comprised of warm silicates only.

decrease in prominence until at 1% corundum, 99% warm silicates the height of the feature is such that the 13/9.7 μm flux ratio is similar to that observed in AGB stars exhibiting the feature. Since only 1% of the dust needs to be corundum in order for its 13 μm feature to be observable, our models suggest that if corundum forms, it will be seen. One of the objections to the attribution of the 13 μm feature to corundum is that it should be accompanied by a weaker feature at $\sim$21 μm that is not seen in observed spectra (Begemann et al. 1997). However, as shown in Figure 1, the 21 μm feature is intrinsically weak, and it has been suggested that this feature would be difficult to observe (Glaccum 1995). This is supported by our models that show that, at low relative abundances, the corundum $\sim$21 μm feature cannot be seen, being well hidden by the silicate features. Figure 5 shows that the 21 μm feature does not appear until the relative abundance of corundum exceeds $\sim$25%. Therefore, we should not rule out corundum as the carrier of the 13 μm feature on these grounds.

Since a dust composition of 99 : 1 silicate to corundum yields a promising spectrum at $\tau_{10\ \mu m} = 0.05$, we have investigated the effect of optical depth variations on the emerging spectra. At low optical depths ($\tau_{10\ \mu m} = 0.05$, 0.1, and 1), the 13 μm feature is visible and at a reasonable intensity (Fig. 6). However, at $\tau_{10\ \mu m} = 5$, the feature goes into absorption. This happens at lower optical depths for higher relative abundances of corundum. The 13 μm feature has never been observed in absorption, limiting the τ versus relative abundance space in the stars that exhibit this feature. Furthermore, this feature is not seen in O-rich evolved stars with very high optical depths (Maldoni et al. 2005), suggesting that high densities may preclude the formation of corundum (if the 13 μm feature is indeed attributable to corundum).

4.2. *Spinel*

In Figure 7, we present the spectra from the spinel models of various relative abundances, again at $\tau_{10\ \mu m} = 0.05$. From this we can see that, in order for the 13 μm feature to appear with the observed strength, it would be necessary to set spinel at $\gtrsim$5% of the dust composition, with warm silicates comprising the remainder. At this relative abundance, there is a clearly observable 17 μm feature. Both Sloan et al. (2003) and Heras & Hony (2005) have shown that this feature does not occur in the *ISO* spectra of AGB stars that exhibit the 13 μm feature.

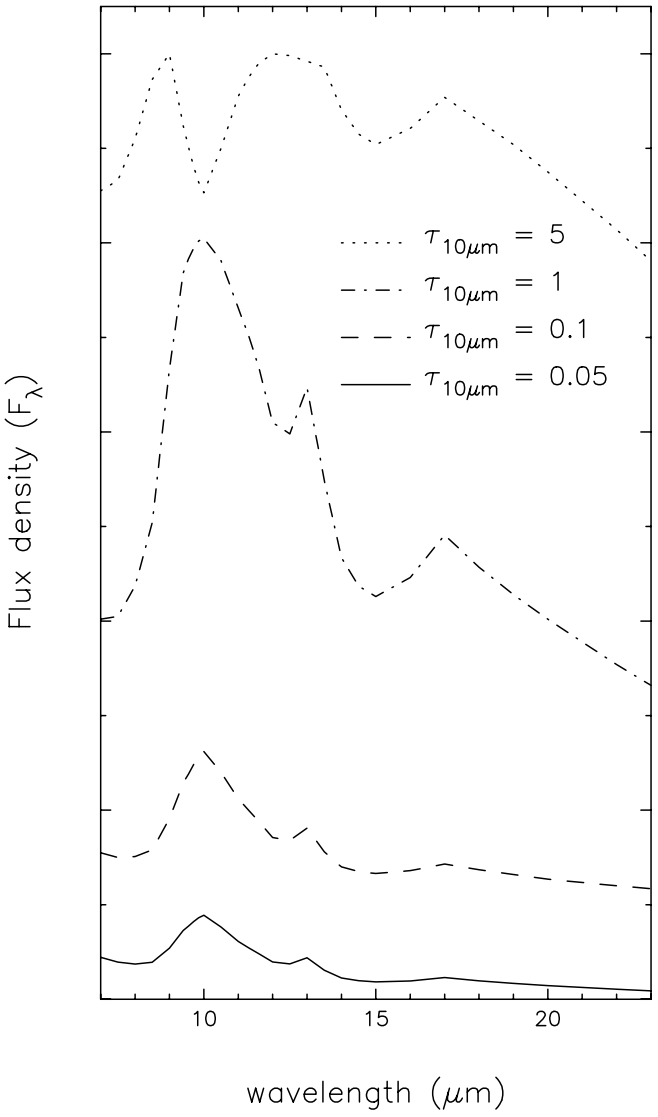

FIG. 8.—Model 7–23 μm spectra for a fixed mixture of spinel (5%) and warm silicates (95%) at different optical depths.

Figure 8 shows the effect of optical depth on the spinel 13 μm feature. In these models the relative abundances are 5% spinel and 95% silicate. In all cases, the models predict a small but noticeable emission feature at 17 μm. Note that this feature is seen in emission even at high optical depth, when the silicate feature is seen in absorption. The 17 μm feature is not seen in *ISO* spectra of AGB stars that exhibit the 13 μm feature. While Posch et al. (1999) suggest that there is a 17 μm feature in their objects' spectra, the observed feature has an FWHM of only 0.15 μm (Sloan et al. 2003), much narrower than the model data for the spinel feature. The DUSTY models for spinel grains confirm this (Fig. 9). The lack of observed 17 μm features rules out spinel as the carrier of the 13 μm feature.

4.3. *Amorphous Alumina*

Figure 10 shows the models in which the dust composition comprises only corundum and amorphous alumina. Even at very low relative abundances (1% corundum, 99% alumina), the corundum 13 μm feature is easily seen. Figure 11 shows the effect of optical depth on these models and demonstrates that the corundum feature is seen at most optical depths. This shows that the introduction of amorphous alumina grains cannot mask the corundum 13 μm feature unless the optical depth is very high. If corundum is present, we will see it.

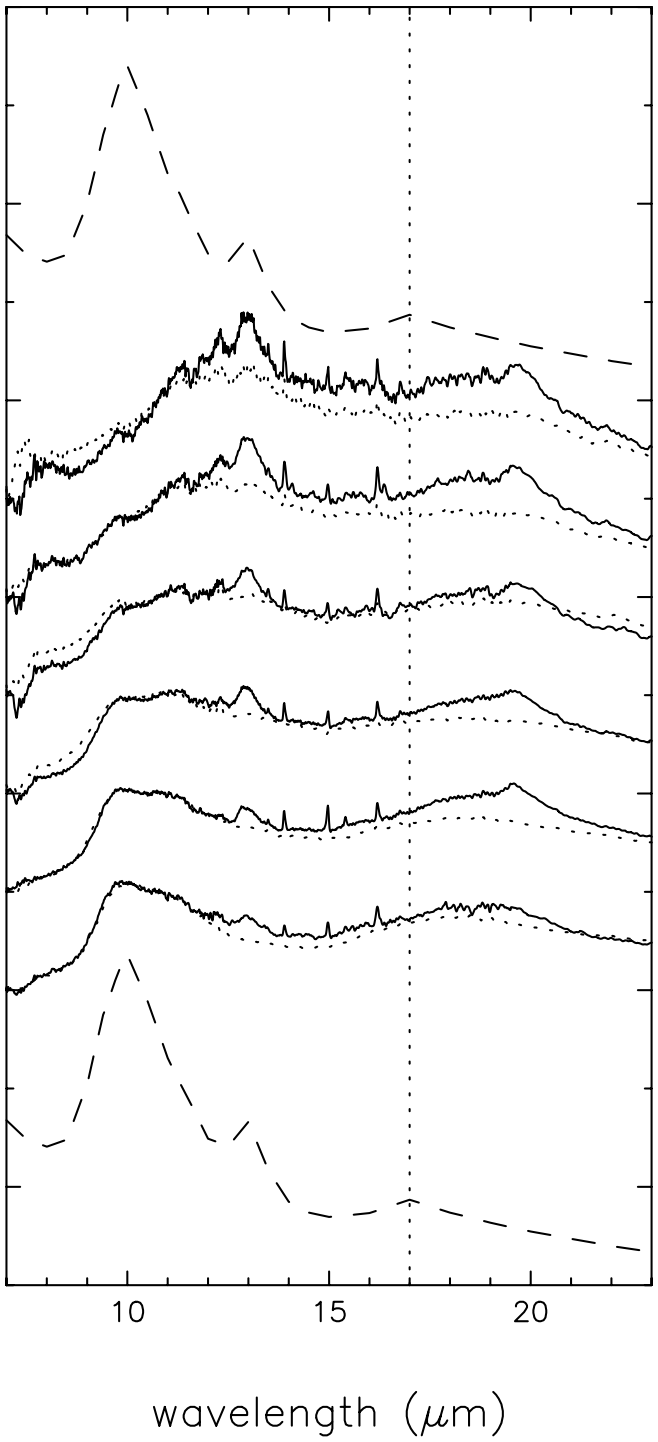

FIG. 9.—Comparison of the 5% spinel mixture at $\tau_{10\ \mu m} = 0.05$ with spectra from stars of different silicate emission indices. The 17 μm feature is marked for clarity.

4.4. *Comparison with ISO SWS Spectra*

By using the spectral classification system developed by Sloan & Price (1995, 1998), Sloan et al. (2003) reinvestigated the observed 13 μm feature using *ISO* SWS observations. Their spectral classification uses the shape/strength of the silicate feature to divide observed spectra into eight categories (designated

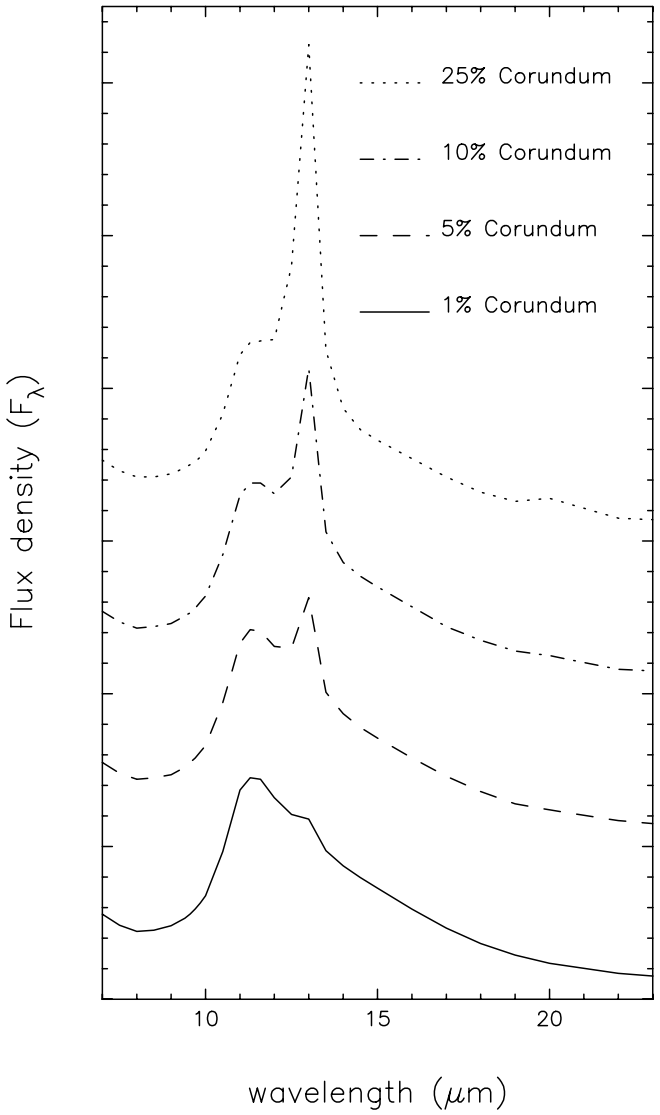

FIG. 10.—Model 7–23 μm spectra of different mixtures of corundum and amorphous alumina at fixed optical depth ($\tau_{10\ \mu m} = 0.05$). In each case the dust composition is given by the percentage of corundum, with the remainder of the dust comprised of amorphous alumina only ($\tau_{10\ \mu m} = 0.05$).

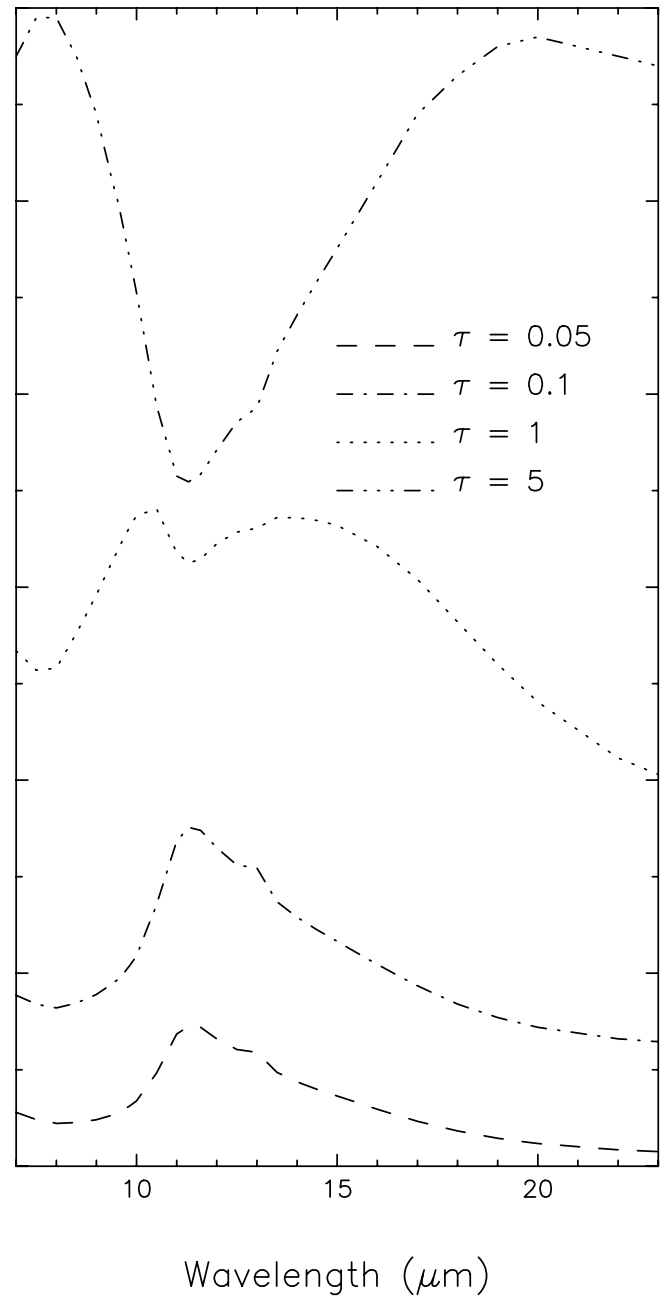

FIG. 11.—Model 7–23 μm spectra for a fixed mixture of corundum (1%) and amorphous alumina (99%) at various optical depths.

by SE#, where # = 1–8; SE8 has the strongest classic silicate feature, SE1, the weakest). Figure 12 compares the continuum-subtracted average spectra for each silicate class (see also Fig. 1 of Sloan et al. 2003) with the spectra exhibiting the 13 μm feature separated from those that do not. This figure shows that the 13 μm feature is strongest in the SE1 class and weakens with increasing SE number. However, as shown in Figure 13, the 9.7/13 μm ratio shows an almost identical trend for the spectra without the 13 μm feature, suggesting that the apparent strengthening of the 13 μm feature is an artifact of the increasing underlying dust emission at this wavelength (probably due to amorphous alumina). We assume that the only difference between the circumstellar shells that exhibit the 13 μm feature and those that do not is that one has an extra component giving rise to the 13 μm (and associated) features. By dividing the spectrum with the feature by the spectrum without for each of the SE classes, we find that the residual spectrum remains constant (see Fig. 14). The strength of the extra 13 μm emission does not change with the SE class. This implies that the relative abundance of the 13 μm carrier remains more or less constant, regardless of the trends in the other spectral features. Figure 15 shows how our models compare to the observations presented in Sloan et al. (2003). For classes SE1 and SE2 the relative abundance of corundum needed to match the strength of the observed 13 μm feature is ~5%–10%. While the 10 μm silicate feature in these classes is weak, it is still clearly present. Amorphous alumina is also necessary to match the shape of the spectrum between 10 and 12 μm. Classes SE3 and SE4 show a similar structure, with a corundum relative abundance in the ~5%–10% range and contributions from both silicates and amorphous alumina. The silicate contribution is stronger than for classes SE1 and SE2. For classes SE5 and SE6, the silicate contribution is much stronger, although some amorphous alumina is still needed to match the shape of the spectrum between 10 and 12 μm. The 13 μm feature now requires ~5% corundum. These models show that the spectra of all 13 μm

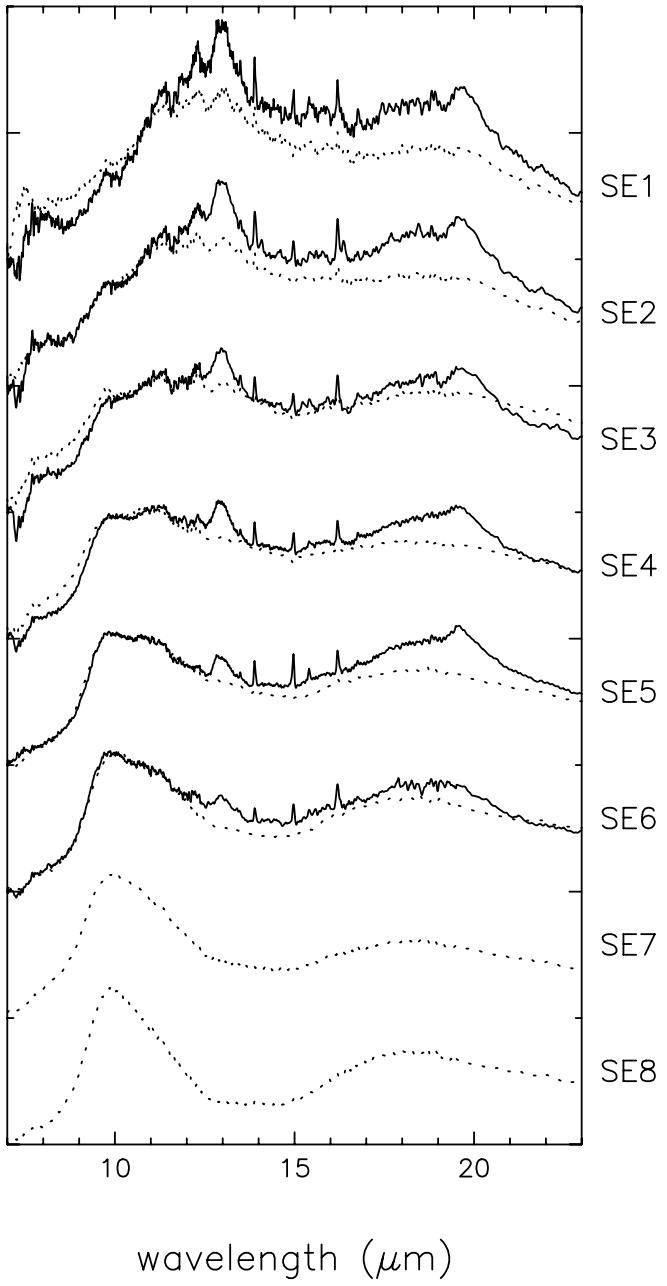

FIG. 12.—Continuum-subtracted *ISO* SWS spectra of O-rich AGB stars that do (*solid line*) or do not (*dotted line*) exhibit the 13 μm feature. For a description of the SE classes, please see § 4.4, Sloan & Price (1995, 1998), and Sloan et al. (2003).

objects are consistent with a relative abundance of corundum of approximately 5%. In all classes (SE1–SE6) the shape of the spectrum between ~8 and ~12 μm can be explained by differing relative abundances of silicate and amorphous alumina.

The most obvious failure of these models is in fitting the 16–22 μm region. The models are not able to account for the strong, broad feature in this region. Even models with a large amount of silicate cannot reproduce this feature. This is discussed further in § 5.

5. DISCUSSION AND CONCLUSIONS

Using DUSTY, we have shown that spinel is unlikely to be the carrier of the 13 μm feature. Its 17 μm feature is too broad to fit observational spectra of AGB stars exhibiting the 13 μm feature (Fig. 9). The narrow observed 17 μm feature is probably

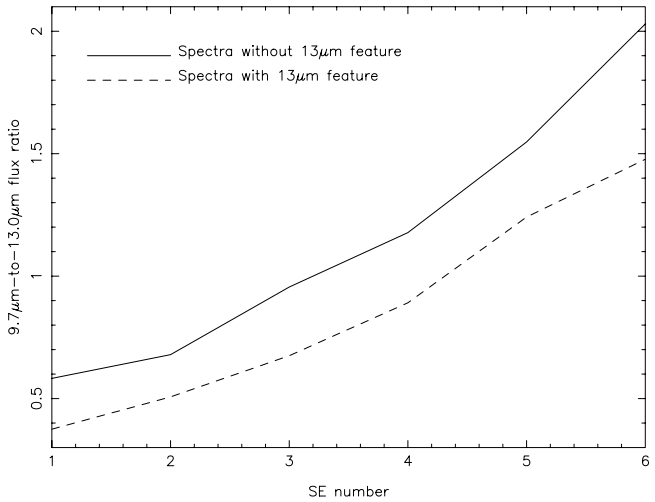

FIG. 13.—Ratios of the 9.7 and 13 μm fluxes as a function of silicate emission index among spectra with (*solid line*) and without (*dashed line*) the 13 μm feature.

produced by CO_2 (Sloan et al. 2003) or some other gaseous component.

Our models suggest that if corundum is present in an AGB dust shell, even at very small relative abundances, it should be observable. The principal argument against corundum was the lack of observation of its 20.5 μm feature (Begemann et al. 1997). At low relative abundances (1% corundum), the 13 μm feature is clearly visible, but the weak 20.5 μm feature is not seen, being effectively hidden by the broad amorphous silicate emission. It is clear from these models that the 20.5 μm feature should not be used to determine the presence or absence of corundum in AGB stars. Corundum is still a viable carrier for the 13 μm feature. Our models suggest that, if corundum is indeed the carrier of the 13 μm feature, it is present at a relative abundance of ~5% for all stars that exhibit the feature.

If corundum is the carrier of the 13 μm feature, we must account for its appearance in many SRs and few Mira variables. Since Mira variables are expected to have higher mass-loss rates, the density of the dust forming region in Mira variables will be higher than in SRs. These high densities may preclude

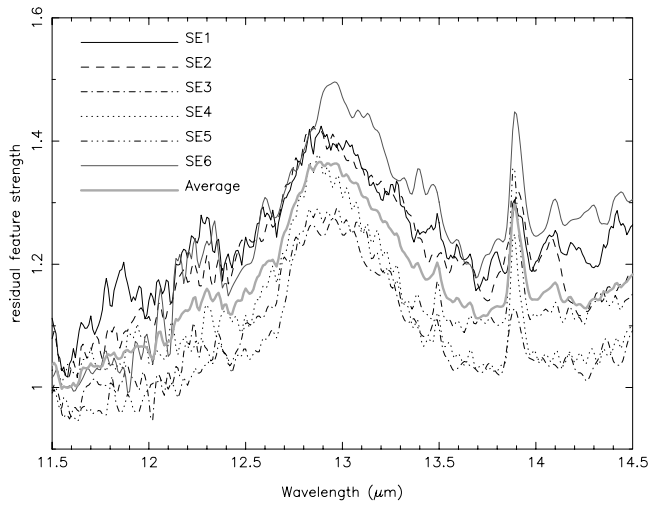

FIG. 14.—Residual spectra. For each silicate emission index, the average spectrum that exhibits the 13 μm feature has been divided by the average spectrum that does not show this feature.

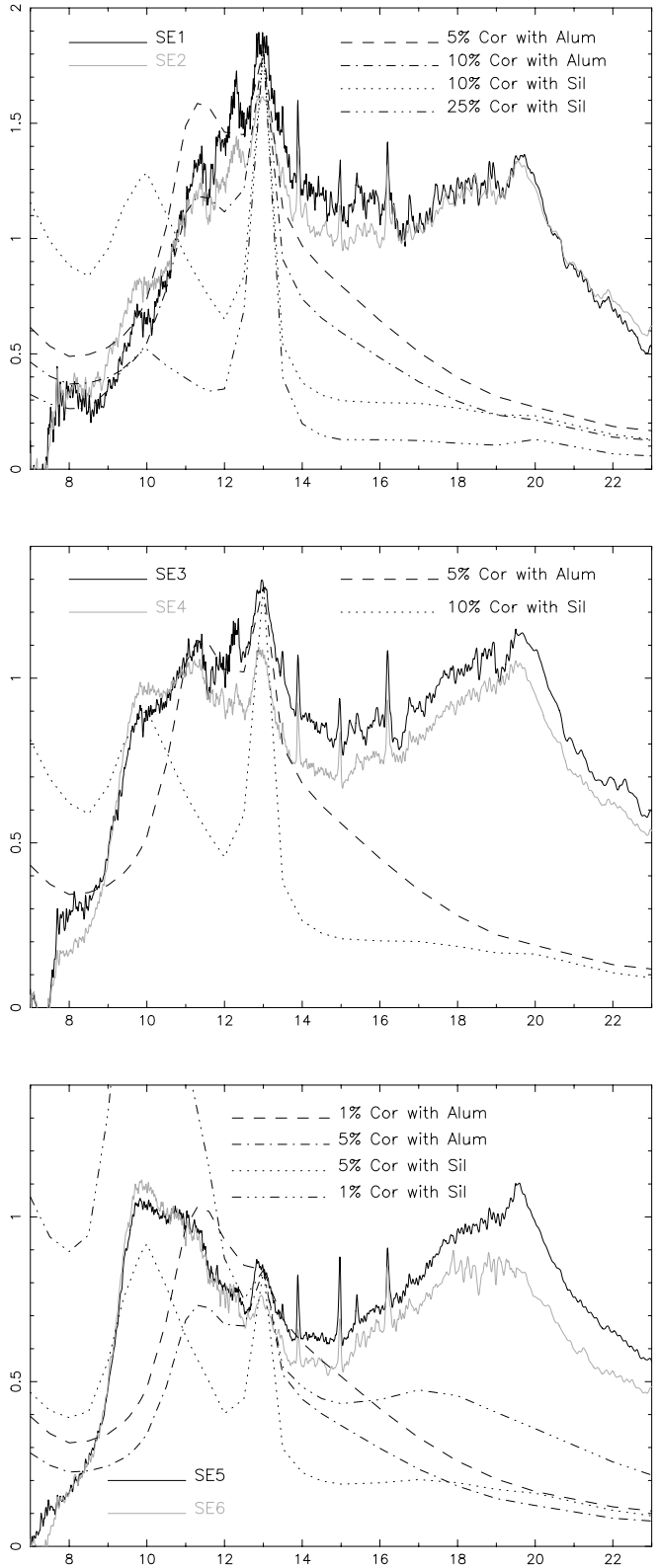

FIG. 15.—Comparison of the corundum models with the continuum-subtracted spectra from stars of different silicate emission indices. For a description of the SE classes, please see § 4.4, Sloan & Price (1995, 1998), and Sloan et al. (2003). *Top*: silicate emission classes SE1 and SE2. *Middle*: silicate emission classes SE3 and SE4. *Bottom*: silicate emission classes SE5 and SE6.

the formation of corundum, instead forming amorphous alumina. However, the models shown in Figure 15 suggest that there is always some amorphous alumina present in these dust shells. The shape of the 10 μm feature in the SE classes is a combination of silicate and amorphous alumina (see also Speck et al. 2000). The occurrence and strength of the 13 μm feature do not correlate with the relative abundance of amorphous alumina. If high densities cause Al_2O_3 to form amorphous rather than crystalline grains, there should be an anticorrelation between the strength of the amorphous alumina feature and that of corundum. As shown in § 4.4, the strength of the 13 μm feature is remarkably constant across all SE classes. Under these circumstances, it is difficult to understand what causes the corundum to be associated with SRs and not with Mira variables. Our models show that even low relative abundances of corundum will give rise to an observable 13 μm feature, so simply making more silicate and/or amorphous alumina will not hide the feature. It is possible that the corundum grains are more effectively coated by silicates in Mira variables, but this must also happen to some extent in SRs, as we expect Al_2O_3 grains to act as seed nuclei for silicate formation (e.g., Salpeter 1974).

It is also clear from Figures 1 and 2 that if corundum or spinel were the carrier of the 13 μm feature, the grains would necessarily be spherical. Any other grain shape moves the 13 μm feature to longer wavelengths than observed. Thus, if corundum or spinel were found to be present predominantly in nonspherical grains, they would not emit at 13 μm and would thus be automatically excluded from this investigation. Further meteoritic studies into the typical grain shape and crystal structure of these minerals in presolar grains would greatly aid us in the identification of the 13 μm carrier.

Previous IR studies of crystalline spinel have found spectral features at wavelengths longward of 13.5 μm (e.g., Chopelas & Hofmeister 1991; Hafner 1961; Preudhomme & Tarte 1971). Indeed, it was these previously published spectra that prompted Speck (1998) to ignore spinel in her discussion of mid-IR dust features because it did not appear to have any features in the 7.5–13.5 μm window and would therefore not be a candidate for the 13 μm feature. These previous studies were for terrestrial samples and imply that for naturally occurring spinel on the Earth, the grains are not spherical in shape. This begs the question, Why should circumstellar environments form only spherical oxide grains? The answer may be as simple as the difference in pressure regimes between terrestrial mineral formation and stardust formation. However, for crystalline minerals, one might expect growth to occur according to the crystal structure, and thus similarities between terrestrial and circumstellar grain shapes may be inevitable.

It has been proposed that grain shape is dependent on the temperature of formation of the grains, with warmer dust forming spherical grains, while species formed in cooler environments tend toward spheroidal formations (Voshchinnikov & Semenov 2000). It is possible that this could explain why corundum (and/or spinel) form spherical grains. This also suggests that corundum (and/or spinel) formation is inhibited at low temperatures because we do not see the features associated with other grain shapes.

The aim of the models presented here is to understand the 13 μm feature; consequently, some other features are not well fitted by our models. In particular, the models presented in § 4 fail to fit the strong, broad feature in the 16–22 μm region. Even models with a large amount of silicate cannot reproduce this feature. It is possible that the emission in the 16–22 μm range is produced by other oxides, i.e., MgO–FeO. These minerals would be expected to form as a by-product of the formation of silica

(SiO_2). The silicates that dominate the spectra of many O-rich AGB stars basically form by reacting SiO_2 with MgO and FeO (e.g., Rietmeijer et al. 1999; Lodders & Fegley 1999). If the reactions reach equilibrium, all these oxides become incorporated into silicates, and there should not be spectral features associated with MgO–FeO or SiO_2. However, if equilibrium is not reached, which may be possible in the less dense SR dust shells, we might expect to have residual SiO_2, MgO, and FeO grains in these circumstellar dust envelopes contributing to the spectrum. These metal oxides form a compositional series of the form $Mg_xFe_{(1-x)}O$ ($0 \leq x \leq 1$). There are spectral features associated with these minerals that occur in the range $\sim$15–25 μm (Henning et al. 1995; Begemann et al. 1995; Hofmeister et al. 2003), with the pure MgO endmember peaking at approximately 25 μm and the pure FeO endmember peaking at approximately 20 μm. The intermediate compositions are reported to have features in the $\sim$15–20 μm range (Begemann et al. 1995). If the strong broad feature(s) seen in the 16–22 μm range is (are) produced by the MgO–FeO minerals, we would also expect to see SiO_2 features, which could potentially explain both the 13 μm feature (and remove the need for corundum grains), and the $\sim$10 μm feature, currently attributed to silicates. Silica may also be responsible for the 28 μm feature discussed by Sloan et al. (2003), as the optical constants of quartz (a polymorph of SiO_2) show that there should be an emission feature at about this wavelength (Spitzer & Kleinman 1961). Detailed modeling and discussion of the silica hypothesis will appear in a forthcoming paper (K. DePew et al. 2006, in preparation).

We would like to thank Greg Sloan for his *ISO* SWS spectra of O-rich AGB stars. This work is supported in part by NASA grant APRA04-0000-0041

REFERENCES

Begemann, B., Dorschner, J., Henning, T., Mutschke, H., Guertler, J., Kömpe, C., & Nass, R. 1997, ApJ, 476, 199
Begemann, B., Henning, T., Mutschke, H., & Dorschner, J. 1995, Planet. Space Sci., 43, 1257
Bohren, C. F., & Huffman, D. R. 1983, Absorption and Scattering of Light by Small Particles (New York: Wiley)
Chopelas, A., & Hofmeister, A. M. 1991, Phys. Chem. Min., 18, 279
Clayton, D., & Nittler, L. 2004, ARA&A, 42, 39
de Graauw, T., et al. 1996, A&A, 315, L49
Dijkstra, C., Speck, A. K., Reid, R. B., & Abrahams, P. 2005, ApJ, 633, L133
Fabian, D., Posch, T., Mutschke, H., Kerschbaum, F., & Dorschner, J. 2001, A&A, 373, 1125
Feast, M. W., & Whitelock, P. A. 1987, in Late Stages of Stellar Evolution, ed. S. Kwok & S. R. Pottasch (Dordrecht: Reidel), 33
Gervais, F. 1991, in Handbook of Optical Constants of Solids, ed. E. D. Palik (Orlando: Academic), 761
Gillett, F. C., Low, F. J., & Stein, W. A. 1968, ApJ, 154, 677
Glaccum, W. 1995, in ASP Conf. Ser. 73, Airborne Astronomy Symp. on the Galactic Ecosystem: From Gas to Stars to Dust, ed. M. R. Haas, J. A. Davidson, & E. F. Erickson (San Francisco: ASP), 395
Hafner, S. 1961, Z. Krist., 115, 331
Heras, A. M., & Hony, S. 2005, A&A, 439, 171
Henning, T., & Mutschke, H. 1997, A&A, 327, 743
Henning, T., et al. 1995, A&AS, 112, 143
Hofmeister, A. M., Keppel, E., & Speck, A. K. 2003, MNRAS, 345, 16
Hoppe, P. 2004, in ASP Conf. Ser. 309, Astrophysics of Dust, ed. A. N. Witt, G. C. Clayton, & B. T. Draine (San Francisco: ASP), 265
Huss, G. R., Fahey, A. J., Gallino, R., & Wasserburg, G. J. 1994, ApJ, 430, L81
Justtanont, K., Feuchtgruber, H., de Jong, T., Cami, J., Waters, L. B. F. M., Yamamura, I., & Onaka, T. 1998, A&A, 330, L17
Kerschbaum, F., & Hron, J. 1992, A&A, 263, 97
Kessler, M. F., et al. 1996, A&A, 315, L27
Kozasa, T., & Sogawa, H. 1997a, Ap&SS, 251, 165
———. 1997b, Ap&SS, 255, 437
Little-Marenin, I. R., & Little, S. J. 1988, ApJ, 333, 305
———. 1990, AJ, 99, 1173
Little-Marenin, I. R., & Price, S. D. 1986, in Summer School on Interstellar Processes: Abstracts of Contributed Papers, ed. D. J. Hollenbach & H. A. Thronson (NASA Tech. Mem. 88342; Moffett Field: NASA), 137
Lodders, K., & Fegley, B. 1999, in IAU Symp. 191, Asymptotic Giant Branch Stars, ed. T. Le Bertre, A. Lèbre, & C. Waelkens (San Francisco: ASP), 279
Maldoni, M. M., Ireland, T. R., Smith, R. G., & Robinson, G. 2005, MNRAS, 362, 872
Marengo, M., Ivezić, Ž., & Knapp, G. R. 2001, MNRAS, 324, 1117
Mathis, J. S., Rumpl, W., & Nordsieck, K. H. 1977, ApJ, 217, 425
Min, M., Hovenier, J. W., & de Koter, A. 2003, A&A, 404, 35
Nenkova, M., Ivezić, Ž., & Elitzur, M. 2000, in ASP Conf. Ser. 196, Thermal Emission Spectroscopy and Analysis of Dust, Disks, and Regoliths, ed. M. L. Sitko, A. L. Sprague, & D. K. Lynch (San Francisco: ASP), 77
Neugebauer, G., et al. 1984, ApJ, 278, L1
Nittler, L. R., Alexander, C. M. O'D., Gao, X., Walker, R. M., & Zinner, E. K. 1994a, Meteoritics, 29, 512
———. 1994b, Nature, 370, 443
———. 1997, ApJ, 483, 475
Onaka, T., de Jong, T., & Willems, F. J. 1989, A&A, 218, 169
Ossenkopf, V., Henning, T., & Mathis, J. S. 1992, A&A, 261, 567
Posch, T., Kerschbaum, F., Mutschke, H., Fabian, D., Dorschner, J., & Hron, J. 1999, A&A, 352, 609
Preudhomme, J., & Tarte, P. 1971, Spectrochim. Acta, 27A, 1817
Ramdani, A. 2003, in Exploiting the *ISO* Data Archive, ed. C. Gry et al. (ESA SP-511; Noordwijk: ESA), 145
Rietmeijer, F. J. M., Nuth, J. A., & Karner, J. M. 1999, ApJ, 527, 395
Rowan-Robinson, M., & Harris, S. 1982, MNRAS, 200, 197
———. 1983a, MNRAS, 202, 767
———. 1983b, MNRAS, 202, 797
Salpeter, E. E. 1974, ApJ, 193, 579
Sedlmayr, E. 1997, Ap&SS, 251, 103
Sloan, G. C., Kraemer, K. E., Goebel, J. H., & Price, S. D. 2003, ApJ, 594, 483
Sloan, G. C., Levan, P. D., & Little-Marenin, I. R. 1996, ApJ, 463, 310
Sloan, G. C., & Price, S. D. 1995, ApJ, 451, 758
———. 1998, ApJS, 119, 141
Speck, A. K. 1998, Ph.D. thesis, Univ. College London
Speck, A. K., Barlow, M. J., Sylvester, R. J., & Hofmeister, A. M. 2000, A&AS, 146, 437
Spitzer, W. G., & Kleinman, D. A. 1961, Phys. Rev., 121, 1324
Stroud, R. M., Nittler, L. R., & Alexander, C. M. O'D. 2004, Science, 305, 1455
Tielens, A. G. G. M. 1990, in From Miras to Planetary Nebulae: Which Path for Stellar Evolution?, ed. M. O. Mennessier & A. Omont (Gif-sur-Yvette: Editions Frontières), 186
Tielens, A. G. G. M., Waters, L. B. F. M., Molster, F. J., & Justtanont, K. 1997, Ap&SS, 255, 415
Vardya, M. S., de Jong, T., & Willems, F. J. 1986, ApJ, 304, L29
Voshchinnikov, N. V., & Semenov, D. A. 2000, Astron. Lett., 26, 679
Woolf, N. J., & Ney, E. P. 1969, ApJ, 155, L181
Zinner, E., Amari, S., Guinness, R., Nguyen, A., Stadermann, F. J., Walker, R. M., & Lewis, R. S. 2003, Geochim. Cosmochim. Acta, 67, 5083